

MM-Pyramid: Multimodal Pyramid Attentional Network for Audio-Visual Event Localization and Video Parsing

Jiashuo Yu, Ying Cheng, Rui-Wei Zhao, Rui Feng*, Yuejie Zhang*
 Fudan University

{jsyu19, chengy18, rwzhao, fengrui, yjzhang}@fudan.edu.cn

Abstract

Recognizing and localizing events in videos is a fundamental task for video understanding. Since events may occur in auditory and visual modalities, multimodal detailed perception is essential for complete scene comprehension. Most previous works attempted to analyze videos from a holistic perspective. However, they do not consider semantic information at multiple scales, which makes the model difficult to localize events in various lengths. In this paper, we present a Multimodal Pyramid Attentional Network (**MM-Pyramid**) that captures and integrates multi-level temporal features for audio-visual event localization and audio-visual video parsing. Specifically, we first propose the attentive feature pyramid module. This module captures temporal pyramid features via several stacking pyramid units, each of them is composed of a fixed-size attention block and dilated convolution block. We also design an adaptive semantic fusion module, which leverages a unit-level attention block and a selective fusion block to integrate pyramid features interactively. Extensive experiments on audio-visual event localization and weakly-supervised audio-visual video parsing tasks verify the effectiveness of our approach.

1. Introduction

Video scene understanding in computer vision is fundamental for many real-world applications and it simulates the information perception process of human brain. According to the researches in cognitive neuroscience [6, 14], human perceives information from multiple modalities to obtain the overall comprehension. Similar to human brains, auditory and visual data can provide complementary cues from different perspectives for machine video understanding.

In recent years, some works [2–4, 7, 11, 21, 27, 28, 31] focus on the synergistic effects between auditory and visual modalities and acquire the joint multimodal representation,

*indicates corresponding authors.

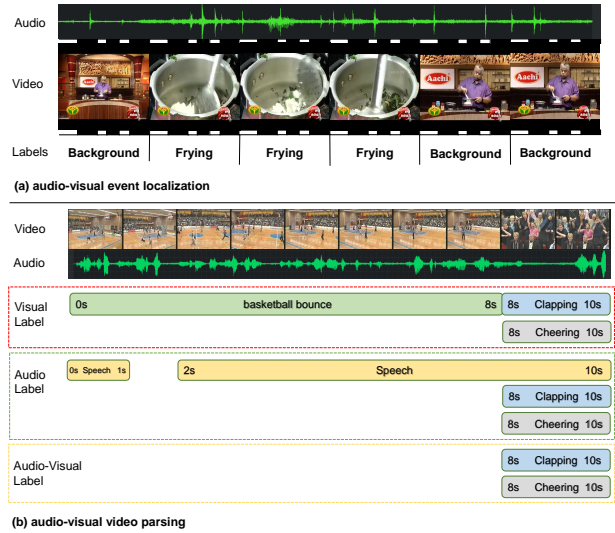


Figure 1. Illustration of the audio-visual event localization and video parsing task. Audio-visual event localization aims to temporally localize a given audio-visual events, while the objective of audio-visual video parsing task is to classify and localize all unimodal and multimodal events in various lengths.

and some other works [1, 18, 50, 51] investigate on localizing sounding objects via self-supervised methods. However, the analysis of audio-visual events in videos, which is a crucial part of the video scene perception, is also in need of investigation. To this end, some tasks and corresponding methods are proposed to explore the impact of audio-visual cues on events. Specifically, Tian et al. [37] propose the audio-visual event localization task, which aims to classify and temporally localize an audio-visual event in a video clip. As shown in Fig. 1(a), the audio-visual event *frying* cannot be seen in the first and last two segments, thereby labeled as *background*. In the other seconds, the food frying can both be heard and seen, thus we label these as *frying*. To make this task more generalizable, Tian et al. [36] expand the task of localizing one event to multiple events scenarios and introduce the audio-visual video parsing task, which is

illustrated in Fig. 1(b), given a video that includes several audible, visible, and audi-visible events, the audio-visual video parsing task aims to predict all event categories, distinguish the modalities perceiving each event, and localize their temporal boundaries. Since the process of labeling all event boundaries is cumbersome, this task is conducted in a weakly-supervised manner, which makes it more generalizable to real-world applications yet more challenging.

Some researchers tackle these problems by capturing contexts from a holistic perspective. For audio-visual event localization, prior works [24, 32, 37, 43–45, 52] explore the relationship between auditory and visual sequences via different kinds of attention mechanisms. For audio-visual video parsing, Tian et al. [36] propose a hybrid attention network to capture the temporal context of the whole video sequence, which tends to focus more on the holistic content and is capable to detect the major event throughout the video. However, these methods are limited by some cases including when the lengths of target events are short, or videos include several events that have various lengths. Since they focus more on the holistic content that is to some extent coarse-grained, detailed information is inclined to be neglected, which makes it difficult to localize short-term events. Despite several methods [41, 46, 49] proposed to capture temporal pyramid features, they can only tackle unimodal scenarios and lack multimodal interactions. Therefore, the necessity of exploring features both in different granularities and modalities emerges, which helps to localize multimodal events in various temporal sizes accurately and further leads to a comprehensive video understanding.

In this paper, we introduce a novel framework called Multimodal Pyramid Attentional Network (**MM-Pyramid**). To be specific, we first propose a novel attentive feature pyramid module composed of multiple pyramid units to acquire multi-level audio-visual features. In each pyramid unit, we introduce a fixed-size multi-scale attention block to capture intra- and inter-modality interactions, together with a dilated convolution block followed to integrate segment-wise features and derive semantic information. To fuse pyramid units, we also design an adaptive semantic fusion module. This module explores the correlations among multi-level features and integrates pyramid units in a selective fusion way. By this means, the model can obtain more targeted joint representation, thereby resulting in better audio-visual event localization and video parsing performance.

In summary, our contributions are as follows:

- We propose to exploit audio-visual pyramid features to learn multi-scale semantic information and localize events in different lengths, which is beneficial for a comprehensive video scene understanding.
- We develop a novel Multimodal Pyramid Attentional

Network, which consists of an attentive feature pyramid module and an adaptive semantic fusion module to capture and integrate multi-level features, respectively.

- We conduct extensive experiments on two audio-visual tasks: audio-visual event localization on the AVE [37] dataset and weakly-supervised audio-visual video parsing on the LLP [36] dataset to verify the effectiveness of our proposed framework.

2. Related Works

Audio-visual representation learning. Audio-visual representation learning aims to acquire the informative multimodal representation by exploiting the correlations between auditory and visual modalities. Some works [2, 4, 7, 11, 21, 27, 28, 31] try to obtain the joint audio-visual representation by learning the correspondence of audio and visual streams in a self-supervised manner. [3, 17] leverage unsupervised clustering as the supervision to explore the cross-modal correlation. Besides, some other works [1, 10, 11, 50, 51] explore the relationship between the sound and dynamic motions of objects and enhance the capability of object localization. In this paper, we try to leverage the correlation between audio and visual content to enhance the performance of downstream applications.

Audio-visual event localization and video parsing. Audio-visual event localization [37] utilizes the synergy and relevance between auditory and visual streams to temporally localize events in the given video. Most prior works [24, 32, 37, 43–45, 47] leverage the attention-based architecture to capture inter- and intra-modality interactions for holistic video understanding. More recently, [52] proposes a positive sample propagation strategy to utilize positive audio-visual pairs, thereby learning discriminative features for the classifier. To expand the event localization task to multi-event scenarios, [36] propose a more generalizable and challenging task named audio-visual video parsing, which aims to classify and locate all audible, visible, and audi-visible events inside a video in a weakly-supervised manner. They also propose a hybrid attention network to capture multimodal contexts and a multimodal multiple instance learning method for the weakly supervised setting. [42] propose to obtain accurate modality-aware event supervision by swapping audio and visual tracks with other unrelated videos to address the modality uncertainty issue. In this paper, we propose to explore multi-scale audio-visual features for localizing events in multiple lengths, which is neglected by previous methods.

3. Task formulation.

Audio-visual event localization aims to classify and localize an audio-visual event in a given video. The task can

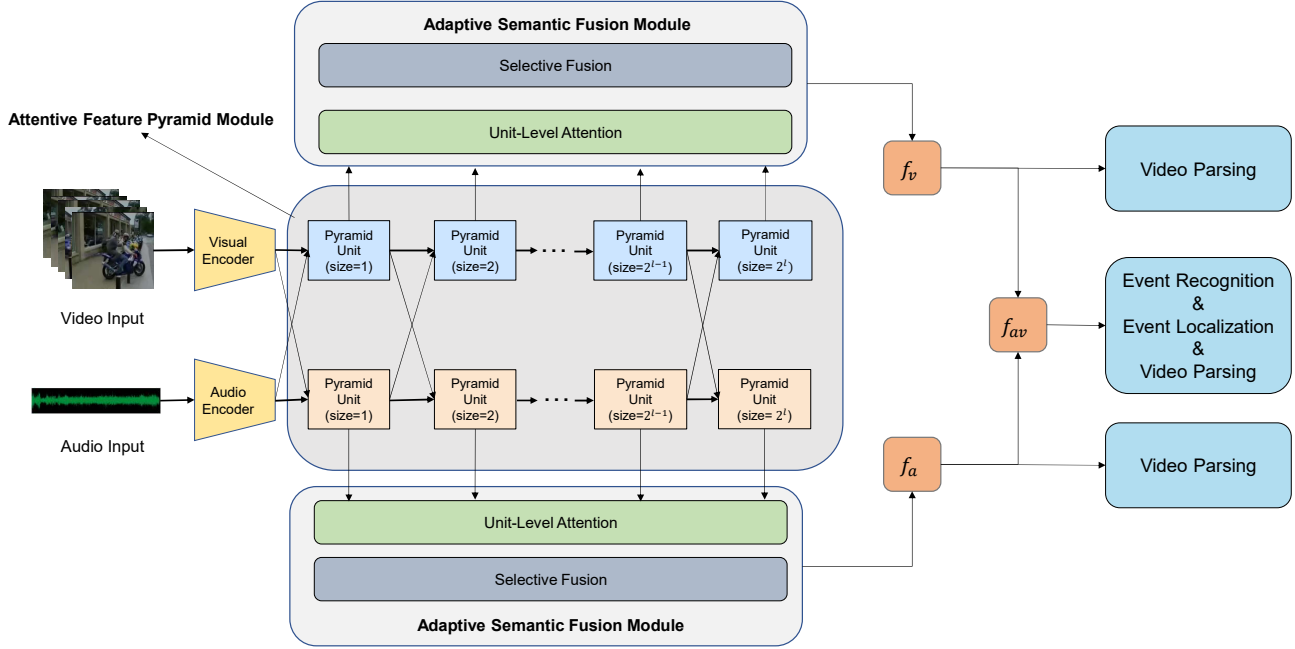


Figure 2. An overview of our proposed Multimodal Pyramid Attentional Network (MM-Pyramid). Multimodal pyramid features are captured by the attentive feature pyramid module, which is composed of multiple pyramid units in different scales. The adaptive semantic fusion module integrates pyramid features via the unit-level attention and the selective fusion operation.

be tackled in fully-supervised and weakly-supervised manners. For fully-supervised manner, the event label for the t_{th} video segment is given as $y_p = \{y_t^p | y_t^p \in \{0, 1\}, p = 1, \dots, C, \sum_{p=1}^C y_t^p = 1\}$, where C is the total number of audio-visual events plus one background category, while in the weakly-supervised setting, only video-level event categories are given during training yet temporal boundaries are still required during inference.

Weakly-supervised audio-visual video parsing aims to predict all event categories, distinguish the modalities perceiving each event, and localize their temporal boundaries. Given a video sequence $\{V_t, A_t\}_{t=1}^N$ with N non-overlapping temporal segments, the event labels are given as $y_t = \{(y_t^v, y_t^a, y_t^{av}) | [y_t^v]^m, [y_t^a]^m, [y_t^{av}]^m \in \{0, 1\}, m = 1, \dots, C\}$, where C is the total number of event categories. An event is labeled as audi-visible only when it is both audible and visible, thus the audi-visible label can be computed as $y_t^{av} = y_t^v * y_t^a$. This task is conducted in a weakly supervised manner. We only have all event categories that appeared in the given video for training, but need to predict which segments contain those events and which modalities perceive them during inference.

4. Methodology

In this section, we introduce our Multimodal Pyramid Attentional Network, which is shown in Fig. 2. We first propose the attentive feature pyramid module to obtain tempo-

ral pyramid features, which is introduced in Sec. 4.1. Then we propose an adaptive semantic fusion module for an interactive pyramid feature fusion in Sec. 4.2, respectively.

4.1. Attentive Feature Pyramid Module

The attentive feature pyramid module is composed of a few stacked units in different scales. Pyramid units in different modalities are connected interactively. The detailed structure of two linked audio and visual pyramid units in the same size are shown in Fig. 3. In each unit, we first propose the fixed-size attention mechanism to introduce intra- and inter-modality interactions, then perform feature integration via a dilated residual convolution block. The size of each unit is different and the outputs of all units are preserved as pyramid-like multimodal features.

Attentive feature interaction. Self-attention (SA) and cross-modal attention (CMA) are used to provide temporal feature interactions. We reform the encoder part of Transformer [39]. Specifically, the attention scores between different video snippets is computed by the scaled dot-product attention $att(q, k, v) = softmax(\frac{qk^T}{\sqrt{d_m}})v$, where q, k, v denotes the query, key, and value vectors, d_m is the dimension of query vectors, T denotes the matrix transpose operation. The self-attention block learns uni-modal temporal relationships via $sa(f) = att(fW_q, fW_k, fW_v)$, where W_q, W_k, W_v are learnable parameters, f is the in-

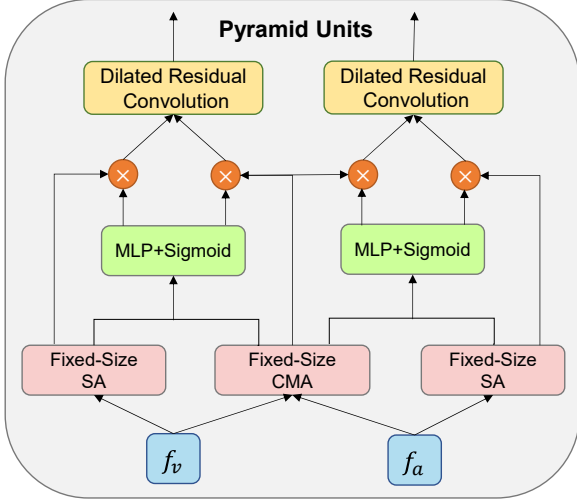


Figure 3. Detailed structure of two linked audio and visual pyramid units in the same level. \times is the channel-wise multiplication. SA and CMA denote self-attention and cross-modal attention.

put feature. For the cross-modal attention block, we assign features in current modality as the query vectors, while the key and value vectors are from features of the other modality. The formulations can be defined as $cma(f_v, f_a) = att(f_v W_q, f_a W_k, f_a W_v)$ and $cma(f_a, f_v) = att(f_a W_q, f_v W_k, f_v W_v)$, where f_a is the audio feature, f_v is the video feature, W_q, W_k , and W_v are learnable parameters. The parameter matrices in the cross-modal attention block are shared. This parameter-efficient setting can project audio and visual features into the same subspaces, which facilitates further interactions of uni-modal and multimodal features. Then the features are processed by a feed-forward layer. We adopt the layer normalization [5] for regularization, and the residual connections [15] for the identity mapping to avoid overfitting.

Since we intend to obtain pyramid features for localizing different lengths of events, the temporal interacting size of each unit ought to be diverse. To this end, we set an interaction window to constrain the interacting size of the self-attention and cross-modal attention layer. Concretely, we propose a fixed-size attention block as shown in Fig. 4, which restricts the interaction windows by adding masks to areas that should not be involved. In this way, the fixed-size attention can be computed as follows,

$$sa(f, d) = att(f W_q, S_t(f, d) W_k, S_t(f, d) W_v), \quad (1)$$

$$cma(f_v, f_a, d) = att(f_v W_q, S_t(f_a, d) W_k, S_t(f_a, d) W_v), \quad (2)$$

$$cma(f_a, f_v, d) = att(f_a W_q, S_t(f_v, d) W_k, S_t(f_v, d) W_v), \quad (3)$$

$$S_t(x, d) = [x_{t-d}, \dots, x_{t+d}], \quad (4)$$

where $S(t)$ indicates creating interaction windows for the t^{th} segment, d denotes the size of the interaction window.

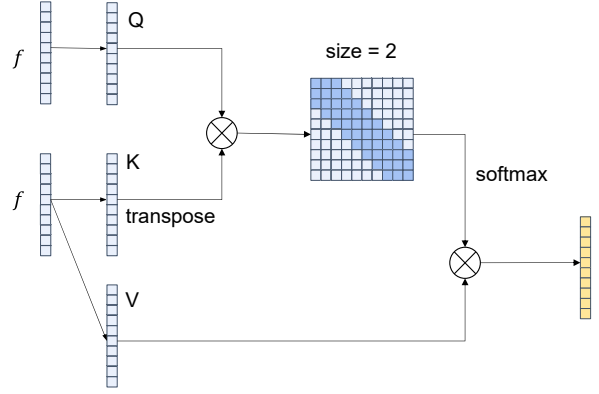


Figure 4. Detailed structure of the fixed-size attention mechanism (the size of the interaction window is 2).

Different from some prior works [7, 36] where self-attention and cross-modal attention blocks are connected in serial, we adopt a parallel arrangement. The inputs of the two kinds of attention blocks are both the output of the previous pyramid unit. We then leverage the channel-wise attention to interconnect and integrate uni-modal and multimodal features. To be specific, the output of self-attention and cross-modal attention blocks are firstly concatenated along the channel dimension. Then channel-wise attention scores are computed to refine raw features via a linear layer followed by a sigmoid function. The final fused features are calculated by the summation of the refined uni-modal and multimodal features. The fusion process of visual modality is formulated as below,

$$F_{fused}^v = \sigma(W_{sa} F_c^v + b_1) F_{sa}^v + \sigma(W_{cma} F_c^v + b_2) F_{cma}^v, \quad (5)$$

$$F_c^v = Concat(F_{sa}^v, F_{cma}^v), \quad (6)$$

where $W_{sa}, W_{cma}, b_1, b_2$ are learnable weights. The formulation of auditory modality fusion is highly similar, thus we omit it for concise writing.

Dilated temporal convolution. Directly utilizing outputs of the fixed-size attention will lead to two problems: First, though interactions among temporal segments have been performed sufficiently, features still need to be amalgamated in temporal dimension to perceive semantic information. Second, since positional encoding is not performed in the attention blocks, temporal order of the sequence has not been modeled, which is important for event understanding. Therefore, a temporal convolution block is used to inject positional information and derive semantic representation.

Temporal convolutional network has been widely applied in speech synthesis [30] and action segmentation [9, 22, 23]. They can provide multi-grained information via multiple dilated convolution layers. The dilation size of each layer is increasing exponentially, which expands the

receptive fields at each layer, thus the network can focus on information in distinct temporal lengths. Following [23], we adopt the dilated residual block for our temporal convolution block. Each dilated residual block contains a 3×3 dilated convolution, a ReLU [13] activation, a 1×1 convolution, and the residual connection. Moreover, instead of causal convolution adopted in some temporal forecasting tasks, we use acausal convolution with kernel size 3 since it can take more contextual information of the current segment into consideration. The operations in each dilated residual block can be described as follows,

$$\hat{F}_t^l = \text{ReLU}(W^1 F_t^l + W^2 F_{t-d}^l + W^3 F_{t+d}^l + b_3), \quad (7)$$

$$\bar{F}_t^l = \hat{F}_t^{l-1} + V * \hat{F}_t^l + b_4, \quad (8)$$

where \bar{F}_t^l is the output of the t -th segment in the l -th pyramid unit, d denotes the dilated size, σ is the ReLU activation, $\{W^i\}_{i=1}^3 \in \mathbb{R}^{D \times D}$ are convolution filter parameters, $b_3 \in \mathbb{R}^D$ is the bias vector, $*$ denotes the 1×1 convolution operation, $V \in \mathbb{R}^{D \times D}$ and $b_4 \in \mathbb{R}^D$ are convolutional weights and bias.

We keep the dilation size of each unit equal to the interactive size of the fixed-size attention mechanism. Besides, the size of each unit is different, thereby guaranteeing that features obtained by these units contain contexts in multiple scales. Finally, we preserve the output of all units $\{F_v^i, F_a^i\}_{i=1}^L$ as the multimodal pyramid features, where L is the total number of pyramid units.

4.2. Adaptive Semantic Fusion Module

A simple way to integrate pyramid features is to conduct pooling over the unit level. However, these pooling methods lack interactions between different levels, resulting in the incompatibility of multi-scale semantic information. To address this problem, we put forward an adaptive semantic fusion module, which consists of a unit-level attention block to explore the correlation of pyramid features and a selective fusion block for adaptively feature integration.

Unit-level attention. Since the interaction size of each pyramid unit is strictly restricted, pyramid units focus on areas in distinct scopes and generate semantic information at different levels, which results in a large semantic gap between pyramid features. To this end, we introduce the unit-level attention to provide contextual interactions and refine the pyramid features. The unit-level attention considers the similarity of contents in different units, and the interacting results vary with the characteristics of the captured features. The interacting process can be formulated as follows,

$$r_t = \text{att}(\bar{F}_t W_q, \bar{F}_t W_k, \bar{F}_t W_v), \quad (9)$$

where $\bar{F}_t \in \mathbb{R}^{L \times D}$ is the outputs of all pyramid units in the t -th segment, W_q, W_k, W_v are learnable parameters.

Selective fusion. Since the type and length of events are uncertain, the model is supposed to pay more attention to features at suitable levels. Therefore, outputs of pyramid units are fused by a selective fusion block after building the relation-aware connections. Specifically, we perform a linear projection on each modality to gain the fusion weights of each unit. By doing so, the selective fusion block can dynamically assign weights on pyramid features in different granularities, and the fusion results vary with the characteristics and the event’s type of the given video. The fused features are computed by the weighted summation,

$$\hat{r}_t = \sum_{l=1}^L w_t^l r_t^l, \quad (10)$$

$$w_t^l = \sigma(W_{sf} r_t^l + b_{sf}), \quad (11)$$

where W_{sf} and b_{sf} denote the linear projection parameters, σ denotes the sigmoid function. We use sigmoid instead of softmax since the characteristics of pyramid features are not mutually exclusive.

Finally, the probabilities in each modality can be computed by the sigmoid and the softmax function for multiple events and single event, respectively. For audio-visual events, since the event is both audible and visible in the same segment, the event probability in the t -th segment p_{av}^t can be computed by the logical conjunction of uni-modal predictions, which is formulated as $p_{av}^t = p_a^t * p_v^t$.

5. Experiments

5.1. Audio-Visual Event Localization

Dataset and metrics. Audio-Visual Event (AVE) [37] dataset is an audio-visual event dataset with 4,183 video clips of 29 classes. Each video clip is 10 seconds with event category annotation per second. We follow the original setting as [37] and divide the dataset as 80%/10%/10% for training, validation, and test, respectively. The overall segment-wise accuracy is used for evaluation, which is the percentage of all matching segments.

Implementation details. Since there is only one audio-visual event in a video, we decompose the task into video-level category predictions and segment-level relevance predictions as prior methods [43, 44, 47] do. Video-level categories are predicted by a temporal average pooling layer followed by a linear classifier, while segment-level relevance predictions are obtained by a segment-wise event-related binary classifier. We employ the VGG-19 [34] network pre-trained on ImageNet [8] and the VGGish [16] network pre-trained on AudioSet [12] for feature extraction. We use Adam [19] as optimizer. The initial learning rate is $2e-5$ and divided by 10 after 50 epochs. We complement more details in Appendix A.

Method	Sup.(%)	W-Sup.(%)
AVE [37]	68.6	66.7
AVDSN [24]	72.6	67.3
DAM [43]	74.5	-
AVRB [33]	74.8	68.9
AVIN [32]	75.2	69.4
CMAN [45]	73.3*	70.4*
AVT [25]	76.8	70.2
MPN [47]	77.6	72.0
CMRAN [44]	77.4	72.9
PSP [52]	77.8	73.5
MM-Pyramid (Ours)	77.8	73.2
MPN on Subset	62.1	53.8
CMRAN on Subset	62.3	54.2
PSP on Subset	62.7	54.4
MM-Pyramid (Ours) on Subset	63.9	55.3

Table 1. Overall accuracy (%) compared with prior methods in both fully and weakly supervised manner. * denotes results re-implemented by the same feature extractor. Subset means the subset of the AVE dataset where events have multiple lengths and do not occur throughout the whole video.

Comparison with the state-of-the-art. We compare our model with all prior methods as shown in Tab. 1. Results show that our model achieves comparable results with the state-of-the-art method PSP [52]. Since more than 60% of events occur throughout the entire video in this dataset, the advantages of our model for detecting events of different lengths are not fully embodied in the full AVE dataset. Therefore, we conduct additional experiments on the subset where events are in multiple lengths. Results show that our model obtains higher performance on the multiple length events subset both in fully and weakly supervised settings. This proves our declaration that our model can detect more events with various lengths via the pyramid setting.

5.2. Audio-Visual Video Parsing

Dataset and metrics. Look, Listen, and Parse (LLP) [36] dataset derived from AudioSet [12] is constructed for the audio-visual video parsing task. It contains 11,849 videos of 25 event categories. Each video clip is 10s long and contains 1.64 events on average. 1,849 videos are randomly sampled to be annotated at the event level for evaluation, where the validation and test set includes 649 and 1,200 videos, respectively. The remaining 10000 videos are annotated in video-level for training. Following [36], we employ the segment-level and event-level F-scores of all modalities as the evaluation metrics. The segment-level metric computes the F-score of each segment, and the event-level metric computes the event-level F-score by comparing the concatenated positive consecutive segments with the event-

Event Type	Methods	Segment Level	Event Level
Audio	Kong et. al 2018 [20]	39.6	29.1
	TALNet [41]	50.0	41.7
	AVE [37]	47.2	40.4
	AVDSN [24]	47.8	34.1
	HAN [36]	60.1	51.3
	Ours	60.9	52.7
	HAN+MA [42]	60.3	53.6
	Ours+MA	61.1	53.8
Visual	STPN [29]	46.5	41.5
	CMCS [26]	48.1	45.1
	AVE [37]	37.1	34.7
	AVDSN [24]	52.0	46.3
	HAN [36]	52.9	48.9
	Ours	54.4	51.8
	HAN+MA [42]	60.0	56.4
	Ours+MA	60.3	56.7
Audio-Visual	AVE [37]	35.4	31.6
	AVDSN [24]	37.1	26.5
	HAN [36]	48.9	43.0
	Ours	50.0	44.4
	HAN+MA [42]	55.1	49.0
	Ours+MA	55.8	49.4
Type@AV	AVE [37]	39.9	35.5
	AVDSN [24]	45.7	35.6
	HAN [36]	54.0	47.7
	Ours	55.1	49.9
	HAN+MA [42]	58.9	53.0
	Ours+MA	59.7	54.1
Event@AV	AVE [37]	41.6	36.5
	AVDSN [24]	50.8	37.7
	HAN [36]	55.4	48.0
	Ours	57.6	50.5
	HAN+MA [42]	57.9	50.6
	Ours+MA	59.1	51.2

Table 2. Audio-visual video parsing F-score results (%) in comparison with recent weakly-supervised methods.

level ground-truth, where the mIOU is set as 0.5. Furthermore, two average metrics Type@AV and Event@AV are also reported. Type@AV means computing the F-score of each event type (audio, visual, and audio-visual) and averaging these results. Event@AV is generated by considering all types of events in each video and computing the composite F-score results.

Implementation details. The outputs of MM-Pyramid p_v^t , p_a^t , and p_{av}^t represent the uni-modal and multimodal parsing results. Since this task is performed in a weakly supervised manner, we follow [36] to leverage an attentive MMIL pooling to generate video-level predictions. We also

Model	Audio		Visual		Audio-Visual		Type@AV		Event@AV	
	Seg	Eve	Seg	Eve	Seg	Eve	Seg	Eve	Seg	Eve
MM-Pyramid-Last	59.6	51.4	53.6	50.1	49.2	43.2	54.1	48.2	56.4	48.6
MM-Unpyramid	59.7	49.6	53.3	50.0	47.7	41.5	53.6	47.0	57.4	48.1
Hybr-Trans w/ PE	60.1	51.9	53.0	50.1	48.4	43.7	54.5	47.6	56.1	48.5
MM-Pyramid w/o conv	60.0	50.8	52.4	49.2	47.9	41.7	53.1	47.0	56.4	47.8
MM-Pyramid w/o residual	60.4	51.5	52.5	49.5	47.7	41.8	53.5	47.6	57.1	48.7
MM-Pyramid w/o ULA	60.6	52.1	53.4	49.8	48.8	43.6	54.3	48.5	56.8	49.2
MM-Pyramid w/o SF	60.5	51.8	53.6	49.9	48.7	43.1	54.3	48.3	56.9	49.1
MM-Pyramid (full)	60.9	52.7	54.4	51.8	50.0	44.4	55.1	49.9	57.6	50.5

Table 3. Ablation studies with different components on the audio-visual video parsing task. We propose several variants to investigate the impact of multimodal pyramid setting, attentive feature pyramid module, and adaptive semantic fusion module.

utilize the label smoothing [35] strategy to alleviate label noises of the weakly supervised setting. Following [36], we employ ResNet-152 [15] and R(2+1)D [38] to extract visual features, and VGGish network to extract audio features. We use the Adam optimizer and set the initial learning rate as $1e-4$, which is degraded by a factor of 5 after 10 epochs. More details are listed in Appendix B.

Comparison with the state-of-the-art. We compare with the state-of-the-art method HAN [36], AVE [37] and AVDSN [24], as well as several competitive weakly supervised event detection methods, which is shown in Tab. 2. To be specific, we choose temporal action localization methods STPN [29] and CMCS [26], sound event detection methods TALNet [40] and [20]. For the new modality-aware method MA [42], since they do not conduct optimization from the network perspective and use the same hybrid attention network (HAN) as [36], our method is not mutually exclusive with their contrastive learning procedure. Therefore, we provide results both using the raw training strategy and the new label refinement and contrastive learning strategy. Results show that our model outperforms all compared networks on all evaluation metrics in a large margin. For the raw training strategy, our model yields up to 2.9% higher on the unimodal metrics (Visual&Event-level) and up to 2.5% higher on the multimodal metrics (Event@AV&Event-level). This proves that the insight of capturing and integrating multimodal pyramid features enables the localization of events in various lengths precisely, which further results in better video parsing performance.

5.3. Ablation Studies

Do pyramid units help? We first investigate the impact of the pyramid units. As shown in Tab. 3, “MM-Pyramid-

Last” means only the output of the last pyramid unit is preserved. “MM-Unpyramid” denotes the sizes of all pyramid units are identical and equal to the size of the last pyramid units in the raw MM-Pyramid framework. “Hybr-Trans w/PE” denotes the 4-layer hybrid transformer encoder with positional encoding. Results show that our full model outperforms all ablated models, indicating the significance of capturing multi-level features via our pyramid settings. We argue that the multimodal information learned by different levels of contexts resolves videos at multiple granularities. We also make comparisons among different transformer-based structures, which are shown in Appendix B.

Does dilated residual convolution help? We also explore the efficacy of our dilated convolution block. “MM-Pyramid w/o conv” indicates that the entire dilated block is removed, “MM-Pyramid w/o residual” means the dilated residual block is replaced with a single 3×3 convolution layer. Without dilated convolution block, the performance declines significantly, showing the integration of pyramid features is necessary for semantics information. The performance also declines when using the vanilla convolution layer, proving that the residual connections and 1×1 convolution can enhance the expressiveness of integrated features.

Does adaptive semantic fusion module help? Multimodal pyramid features are fused interactively. To reveal the contribution of our adaptive semantic fusion module, we propose two ablated models “MM-Pyramid w/o ULA” and “MM-Pyramid w/o SF”. The first model is constructed by removing the unit-level attention, while the other fuses pyramid features via an average pooling layer instead of the selective fusion block. The performance of “MM-Pyramid w/o ULA” declines, which indicates that building

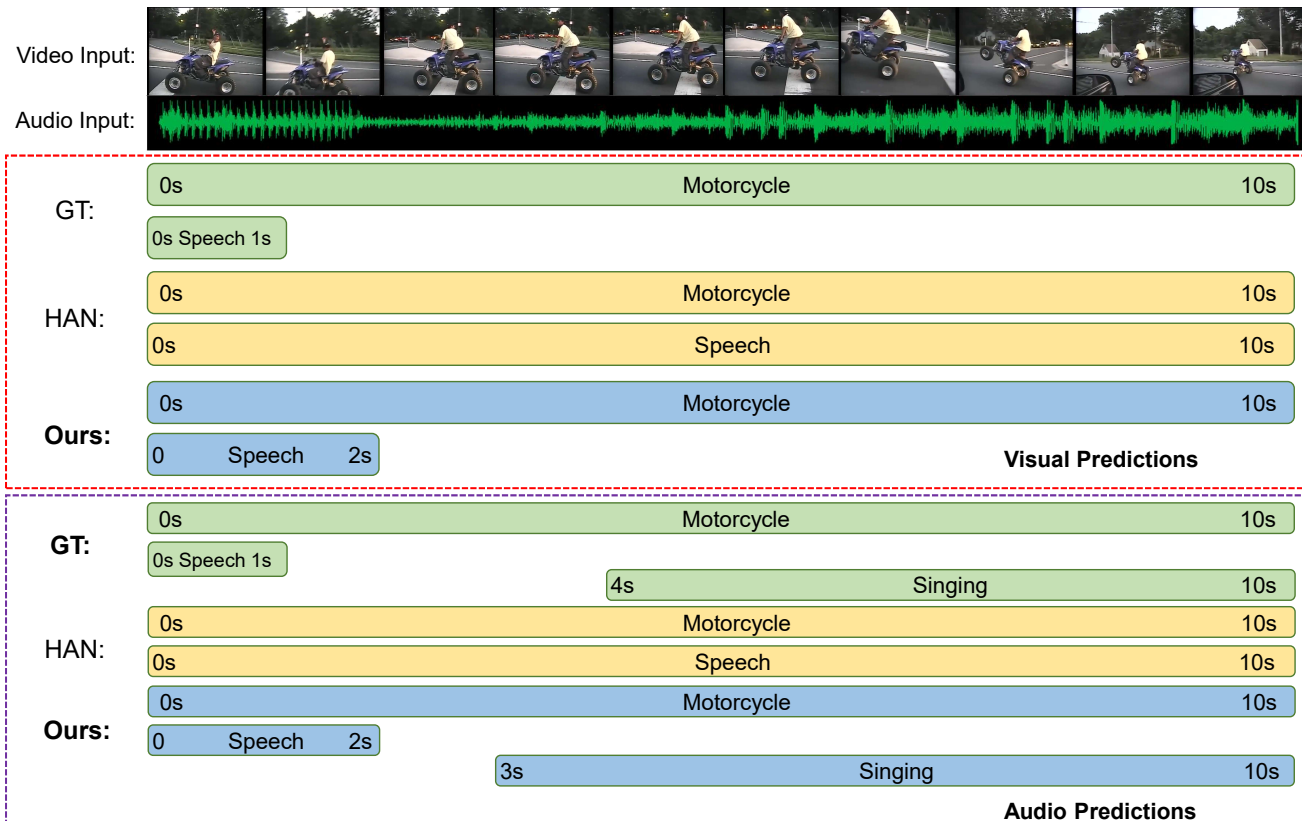


Figure 5. Qualitative comparison with the weakly-supervised audio-visual video parsing method HAN. The red dotted box includes the visual predictions, and the audio predictions are in the purple dotted box. The green, yellow, and blue labels denote the ground-truth, predictions of HAN, and predictions of our MM-Pyramid, respectively.

the relation-aware connections of multi-scale features is effective. Our model also outperforms “MM-Pyramid w/o SF”. We argue that this proves the insight of integrating pyramid features selectively helps the acquisition of complete video scene understanding.

5.4. Qualitative Results

We provide some visualization results to show the effectiveness of our model in capturing multiple events. As shown in Fig. 5, we conduct qualitative experiments on the audio-visual video parsing task in comparison with HAN [36]. The green labels are the ground-truths, and the yellow and blue labels indicate the predictions of HAN and our model, respectively. We found that though the HAN model can precisely predict events that exist throughout the whole video, it fails to detect a short-term event (singing audio events from 4th to 10th seconds) and predicts incorrect event temporal boundary (the speech event in the first second). However, our MM-Pyramid model tends to recognize all events of different sizes and provide predictions with only small deviations (one-second errors in speech and singing events). This result reveals that our model is capable

of exploring features in different granularities, which further leads to localizing events in various lengths precisely. We provide more qualitative results in Appendix D.

6. Conclusion

In this paper, we propose a novel Multimodal Pyramid Attentional Network (MM-Pyramid) for audio-visual event localization and weakly-supervised audio-visual video parsing. Our model captures and integrates multimodal pyramid features in distinct temporal scales for comprehensive scene understanding. To acquire features in different granularities, we propose a novel attentive feature pyramid module, which is composed of the fixed-size attention mechanism and dilated convolution block. Furthermore, we propose an adaptive semantic fusion module to refine and fuse pyramid features in an interactive and selective way. Extensive experiments on the AVE and LLP datasets demonstrate the effectiveness of our proposed approach on localizing events in multiple lengths.

References

- [1] Triantafyllos Afouras, Andrew Owens, Joon Son Chung, and Andrew Zisserman. Self-supervised learning of audio-visual objects from video. In *ECCV*, 2020. 1, 2
- [2] Jean-Baptiste Alayrac, Adrià Recasens, Rosalia Schneider, Relja Arandjelović, Jason Ramapuram, Jeffrey De Fauw, Lucas Smaira, Sander Dieleman, and Andrew Zisserman. Self-supervised multimodal versatile networks. *arXiv preprint arXiv:2006.16228*, 2020. 1, 2
- [3] Humam Alwassel, Dhruv Mahajan, Bruno Korbar, Lorenzo Torresani, Bernard Ghanem, and Du Tran. Self-supervised learning by cross-modal audio-video clustering. In *NeurIPS*, volume 33, 2020. 1, 2
- [4] Relja Arandjelovic and Andrew Zisserman. Look, listen and learn. In *ICCV*, pages 609–617, 2017. 1, 2
- [5] Jimmy Lei Ba, Jamie Ryan Kiros, and Geoffrey E Hinton. Layer normalization. *arXiv preprint arXiv:1607.06450*, 2016. 4
- [6] David A Bulkin and Jennifer M Groh. Seeing sounds: visual and auditory interactions in the brain. *Current opinion in neurobiology*, 16(4):415–419, 2006. 1
- [7] Ying Cheng, Ruize Wang, Zhihao Pan, Rui Feng, and Yuejie Zhang. Look, listen, and attend: Co-attention network for self-supervised audio-visual representation learning. In *ACM MM*, pages 3884–3892, 2020. 1, 2, 4
- [8] Jia Deng, Wei Dong, Richard Socher, Li-Jia Li, Kai Li, and Li Fei-Fei. Imagenet: A large-scale hierarchical image database. In *CVPR*, pages 248–255, 2009. 5
- [9] Yazan Abu Farha and Jurgen Gall. Ms-tcn: Multi-stage temporal convolutional network for action segmentation. In *CVPR*, pages 3575–3584, 2019. 4
- [10] Chuang Gan, Deng Huang, Hang Zhao, Joshua B Tenenbaum, and Antonio Torralba. Music gesture for visual sound separation. In *CVPR*, pages 10478–10487, 2020. 2
- [11] Chuang Gan, Hang Zhao, Peihao Chen, David Cox, and Antonio Torralba. Self-supervised moving vehicle tracking with stereo sound. In *ICCV*, pages 7053–7062, 2019. 1, 2
- [12] Jort F Gemmeke, Daniel PW Ellis, Dylan Freedman, Aren Jansen, Wade Lawrence, R Channing Moore, Manoj Plakal, and Marvin Ritter. Audio set: An ontology and human-labeled dataset for audio events. In *ICASSP*, pages 776–780, 2017. 5, 6, 13
- [13] Xavier Glorot, Antoine Bordes, and Yoshua Bengio. Deep sparse rectifier neural networks. In *Proceedings of the fourteenth international conference on artificial intelligence and statistics*, pages 315–323, 2011. 5
- [14] Aviva I Goller, Leun J Otten, and Jamie Ward. Seeing sounds and hearing colors: an event-related potential study of auditory–visual synesthesia. *Journal of cognitive neuroscience*, 21(10):1869–1881, 2009. 1
- [15] Kaiming He, Xiangyu Zhang, Shaoqing Ren, and Jian Sun. Deep residual learning for image recognition. In *CVPR*, pages 770–778, 2016. 4, 7
- [16] Shawn Hershey, Sourish Chaudhuri, Daniel PW Ellis, Jort F Gemmeke, Aren Jansen, R Channing Moore, Manoj Plakal, Devin Platt, Rif A Saurous, Bryan Seybold, et al. Cnn architectures for large-scale audio classification. In *ICASSP*, pages 131–135, 2017. 5
- [17] Di Hu, Feiping Nie, and Xuelong Li. Deep multimodal clustering for unsupervised audiovisual learning. In *CVPR*, pages 9248–9257, 2019. 2
- [18] Di Hu, Rui Qian, Minyue Jiang, Xiao Tan, Shilei Wen, Errui Ding, Weiyao Lin, and Dejing Dou. Discriminative sounding objects localization via self-supervised audiovisual matching. In *NeurIPS*, volume 33, 2020. 1
- [19] Diederik P Kingma and Jimmy Ba. Adam: A method for stochastic optimization. *arXiv preprint arXiv:1412.6980*, 2014. 5
- [20] Qiuqiang Kong, Yong Xu, Wenwu Wang, and Mark D Plumbley. Audio set classification with attention model: A probabilistic perspective. In *ICASSP*, pages 316–320, 2018. 6, 7
- [21] Bruno Korbar, Du Tran, and Lorenzo Torresani. Cooperative learning of audio and video models from self-supervised synchronization. In *NeurIPS*, page 7774–7785, 2018. 1, 2
- [22] Colin Lea, Michael D Flynn, Rene Vidal, Austin Reiter, and Gregory D Hager. Temporal convolutional networks for action segmentation and detection. In *CVPR*, pages 156–165, 2017. 4
- [23] Shi-Jie Li, Yazan AbuFarha, Yun Liu, Ming-Ming Cheng, and Juergen Gall. Ms-tcn++: Multi-stage temporal convolutional network for action segmentation. *TPAMI*, 2020. 4, 5
- [24] Yan-Bo Lin, Yu-Jhe Li, and Yu-Chiang Frank Wang. Dual-modality seq2seq network for audio-visual event localization. In *ICASSP*, pages 2002–2006, 2019. 2, 6, 7
- [25] Yan-Bo Lin and Yu-Chiang Frank Wang. Audiovisual transformer with instance attention for audio-visual event localization. In *ACCV*, 2020. 6
- [26] Daochang Liu, Tingting Jiang, and Yizhou Wang. Completeness modeling and context separation for weakly supervised temporal action localization. In *CVPR*, pages 1298–1307, 2019. 6, 7
- [27] Shuang Ma, Zhaoyang Zeng, Daniel McDuff, and Yale Song. Active contrastive learning of audio-visual video representations. In *ICLR*, 2021. 1, 2
- [28] Pedro Morgado, Yi Li, and Nuno Nvasconcelos. Learning representations from audio-visual spatial alignment. In *NeurIPS*, volume 33, 2020. 1, 2
- [29] Phuc Nguyen, Ting Liu, Gautam Prasad, and Bohyung Han. Weakly supervised action localization by sparse temporal pooling network. In *CVPR*, pages 6752–6761, 2018. 6, 7
- [30] Aaron van den Oord, Sander Dieleman, Heiga Zen, Karen Simonyan, Oriol Vinyals, Alex Graves, Nal Kalchbrenner, Andrew Senior, and Koray Kavukcuoglu. Wavenet: A generative model for raw audio. *arXiv preprint arXiv:1609.03499*, 2016. 4
- [31] Andrew Owens and Alexei A Efros. Audio-visual scene analysis with self-supervised multisensory features. In *ECCV*, pages 631–648, 2018. 1, 2
- [32] Janani Ramaswamy. What makes the sound?: A dual-modality interacting network for audio-visual event localization. In *ICASSP*, pages 4372–4376, 2020. 2, 6

- [33] Janani Ramaswamy and Sukhendu Das. See the sound, hear the pixels. In *WACV*, pages 2970–2979, 2020. 6
- [34] Karen Simonyan and Andrew Zisserman. Very deep convolutional networks for large-scale image recognition. *arXiv preprint arXiv:1409.1556*, 2014. 5
- [35] Christian Szegedy, Vincent Vanhoucke, Sergey Ioffe, Jon Shlens, and Zbigniew Wojna. Rethinking the inception architecture for computer vision. In *CVPR*, pages 2818–2826, 2016. 7
- [36] Yapeng Tian, Dingzeyu Li, and Chenliang Xu. Unified multisensory perception: Weakly-supervised audio-visual video parsing. In *ECCV*, 2020. 1, 2, 4, 6, 7, 8, 11
- [37] Yapeng Tian, Jing Shi, Bochen Li, Zhiyao Duan, and Chenliang Xu. Audio-visual event localization in unconstrained videos. In *ECCV*, pages 247–263, 2018. 1, 2, 5, 6, 7, 11, 13
- [38] Du Tran, Heng Wang, Lorenzo Torresani, Jamie Ray, Yann LeCun, and Manohar Paluri. A closer look at spatiotemporal convolutions for action recognition. In *CVPR*, pages 6450–6459, 2018. 7
- [39] Ashish Vaswani, Noam Shazeer, Niki Parmar, Jakob Uszkoreit, Llion Jones, Aidan N Gomez, Łukasz Kaiser, and Illia Polosukhin. Attention is all you need. In *NeurIPS*, pages 5998–6008, 2017. 3
- [40] Yun Wang, Juncheng Li, and Florian Metze. A comparison of five multiple instance learning pooling functions for sound event detection with weak labeling. In *ICASSP*, pages 31–35, 2019. 7
- [41] Yunbo Wang, Mingsheng Long, Jianmin Wang, and Philip S Yu. Spatiotemporal pyramid network for video action recognition. In *CVPR*, pages 1529–1538, 2017. 2, 6
- [42] Yu Wu and Yi Yang. Exploring heterogeneous clues for weakly-supervised audio-visual video parsing. In *CVPR*, pages 1326–1335, 2021. 2, 6, 7
- [43] Yu Wu, Linchao Zhu, Yan Yan, and Yi Yang. Dual attention matching for audio-visual event localization. In *ICCV*, pages 6292–6300, 2019. 2, 5, 6
- [44] Haoming Xu, Runhao Zeng, Qingyao Wu, Mingkui Tan, and Chuang Gan. Cross-modal relation-aware networks for audio-visual event localization. In *ACM MM*, 2020. 2, 5, 6
- [45] Hanyu Xuan, Zhenyu Zhang, Shuo Chen, Jian Yang, and Yan Yan. Cross-modal attention network for temporal inconsistent audio-visual event localization. In *AAAI*, volume 34, pages 279–286, 2020. 2, 6
- [46] Ceyuan Yang, Yinghao Xu, Jianping Shi, Bo Dai, and Bolei Zhou. Temporal pyramid network for action recognition. In *CVPR*, pages 591–600, 2020. 2
- [47] Jiashuo Yu, Ying Cheng, and Rui Feng. Mpn: Multimodal parallel network for audio-visual event localization. *ICME*, 2021. 2, 5, 6
- [48] Manzil Zaheer, Guru Guruganesh, Kumar Avinava Dubey, Joshua Ainslie, Chris Alberti, Santiago Ontanon, Philip Pham, Anirudh Ravula, Qifan Wang, Li Yang, et al. Big bird: Transformers for longer sequences. In *NeurIPS*, 2020. 13
- [49] Da Zhang, Xiyang Dai, and Yuan-Fang Wang. Dynamic temporal pyramid network: A closer look at multi-scale modeling for activity detection. In *ACCV*, pages 712–728, 2018. 2
- [50] Hang Zhao, Chuang Gan, Wei-Chiu Ma, and Antonio Torralba. The sound of motions. In *ICCV*, pages 1735–1744, 2019. 1, 2
- [51] Hang Zhao, Chuang Gan, Andrew Rouditchenko, Carl Vondrick, Josh McDermott, and Antonio Torralba. The sound of pixels. In *ECCV*, September 2018. 1, 2
- [52] Jinxing Zhou, Liang Zheng, Yiran Zhong, Shijie Hao, and Meng Wang. Positive sample propagation along the audio-visual event line. In *CVPR*, 2021. 2, 6

A. Experimental Details

In this section, we complement more experimental details, including detailed hyperparameter settings of our MM-Pyramid network, together with the network architecture and training strategy of each task.

A.1. MM-Pyramid

Since we adopt the exponential growth strategy for the size of the pyramid units (experiments on different types of growth strategies can be found in Appendix B.1), the size will continue to expand until it reaches or exceeds the time limit of the video sequence. In the audio-visual localization and video parsing tasks, videos are all 10 seconds clips and features are extracted in the second level. Therefore, the size of each unit is 1, 2, 4, 8, and the unit number L is 4. The hidden size of the feed-forward layer in the transformer block is 512, and the dimensions of all other hidden layers are also 512. The head number of the multi-head attention block is 8.

A.2. Audio-Visual Event Localization

A.2.1 Architectural details

The network architecture of the audio-visual event localization task is shown in Fig. 6(a). For the input features, the 2D visual features are first refined by the audio-guided visual attention [37]. Then the refined visual features and audio features are put into the MM-Pyramid network. Since there only remains one event in the given video, this task can be decomposed into two parts: video-level event category prediction and segment-level event-related prediction. For the former part, the output features of visual and auditory modalities are first concatenated across the channel dimension, then fused by the temporal average pooling. For the latter part, we transform the event category prediction of each segment into the event-related binary prediction. The model only needs to predict whether the current segment belongs to the background category. Finally, we assign the event-related segments with labels of video-level category, and assign the event-unrelated segments with “background”.

A.2.2 Training details

We adopt the cross-entropy loss as the objective function and use gradient clipping during training. The batch size is set to be 32, and we train the model on an NVIDIA Tesla P40 GPU for 500 epochs. To extract visual features, we uniformly pick 16 frames with each second and compute the average results as the visual features. The dimension of the visual feature is $7 \times 7 \times 512$, and the audio feature has a size of 128.

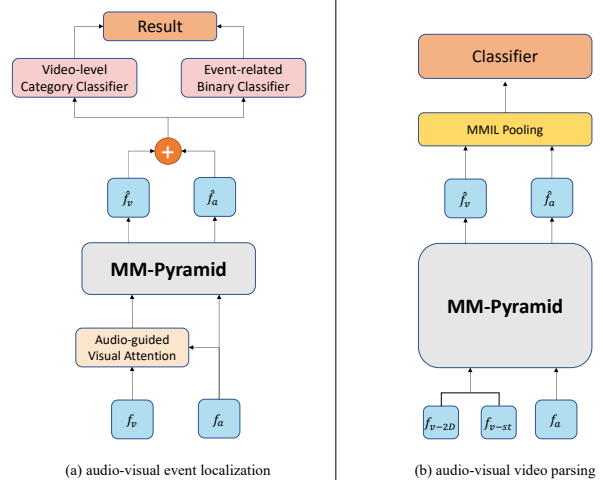


Figure 6. Illustration of the downstream architectures on the audio-visual event localization and weakly-supervised audio-visual video parsing tasks.

A.3. Audio-Visual Video Parsing

A.3.1 Architectural details

To solve the audio-visual video parsing task in a weakly-supervised manner, we follow [36] to leverage an attentive MMIL pooling and generate video-level predictions, which is formulated as:

$$\bar{p} = \sum_{t=1}^T \sum_{m=1}^M (W_{tp} \odot W_{av} \odot P)[t, m, :], \quad (12)$$

$$W_{tp}[:, m, c] = \text{softmax}(F_{tp}[:, m, c]), \quad (13)$$

$$W_{av}[t, :, c] = \text{softmax}(F_{av}[t, :, c]), \quad (14)$$

where m denotes the modality index; W_{tp} and W_{av} are temporal and modality attention parameters; P denotes the stacking of p_a and p_v ; \odot denotes the Hadamard product, F_{tp} and F_{av} are two tensors, which are first stacked by f_a and f_v , and then projected by two fully-connected layers.

To relieve the modality bias of the MMIL problem, unimodal supervisions are added explicitly by a guided loss:

$$\mathcal{L} = \mathcal{L}_g + \mathcal{L}_{wsl}, \quad (15)$$

$$\mathcal{L}_{wsl} = CE(\bar{p}_a, \bar{y}_a) + CE(\bar{p}_v, \bar{y}_v), \quad (16)$$

$$\mathcal{L}_g = CE(\bar{p}, \bar{y}), \quad (17)$$

where CE denotes the cross-entropy loss; \bar{y}_v , \bar{y}_a , and \bar{y} are visual, audio, and audio-visual ground-truths; \bar{p}_v and \bar{p}_a are video-level visual and auditory event predictions, respectively. We also use the label smoothing strategy to alleviate label noises.

A.3.2 Training details.

We use the BCELoss for training. The entire model is trained on a Tesla P40 GPU for 40 epochs with a batch size of 16. We sample visual frames at 8 fps with non-overlapping.

B. Additional Experiments

B.1. Growth strategy of pyramid unit size

We first investigate the effect of different size growth strategies. Despite the exponential growth strategy, we also propose two variant models with a fixed-stride increasing strategy. The strides of two variants are set to be 3 and 4, thus the unit sizes will be 1, 4, 7, 10 and 1, 5, 9, 10, respectively. To constrain the parameters to be the same (which means setting the unit number to 4), we do not adopt other strides. As shown in Tab. 4, our raw model with exponential growth achieves slightly worse results compared with the variant with a stride of 3, and performs better than the other variants. We argue that the 3-stride variant has the most uniform size distribution, while the 4-stride variant obtains uneven granularity distribution. However, when temporal size is extremely large, exponentially increasing allows amplifying the receptive field rapidly while keeping the network shallow, thereby greatly reducing computational overhead. Therefore, the exponential growth strategy is more practical than other strategies.

Table 4. Comparison of different growth strategies of pyramid unit size on the audio-visual video parsing task.

Growth Strategy	Type@AV		Event@AV	
	Segment	Event	Segment	Event
1, 2, 4, 8 (ours)	55.1	49.9	57.6	50.5
F 1, 4, 7, 10 (stride=3)	55.2	49.7	58.4	50.2
1, 5, 9, 10 (stride=4)	53.3	57.0	47.2	48.2

B.2. Acausal convolution vs casual convolution

In the original temporal convolution network (TCN), causal convolution is used as the basic convolution operation, which means only features before the current time step will be taken into consideration. The reason is that TCN was originally applied in some temporal forecasting tasks, and features after the current temporal step should not be available in these tasks. However, we adopt the acausal convolution and take all context information into account. As shown in Tab. 5, the model with casual convolution performs worse than our raw model. This is because the casual convolution will lose all feature information after the current step. In tasks that do not have strict requirements on temporal order, such as event recognition and audio-visual

video parsing, the use of acausal convolution takes more information into account, thereby achieving better performance.

Table 5. Comparison of causal and acausal convolution on the audio-visual video parsing task.

Growth Strategy	Type@AV		Event@AV	
	Segment	Event	Segment	Event
acausal convolution	54.7	49.4	57.4	50.0
causal convolution	55.1	49.9	57.6	50.5

B.3. Impact of channel-attentional refinement

In the pyramid unit, we adopt a parallel arrangement for the self-attention and cross-modal attention blocks, and leverage channel-wise attention to interconnect the unimodal and multimodal features. Here we conduct additional ablation studies to investigate the impact of our design. The ablated model “serial arrangement” denotes self-attention and cross-modal attention blocks are arranged in serial order. The “parallel arrangement w/o channel-attention” denotes removing the channel-wise attention of our raw MM-Pyramid module. Results showed in Tab. 6 show that our raw model outperforms ablated models, showing the effectiveness of our parallel arrangement and the channel-wise attention mechanism.

Table 6. Ablation studies on the impact of channel-wise attention.

Model	Type@AV		Event@AV	
	Segment	Event	Segment	Event
serial arrangement	53.4	48.7	56.5	48.7
parallel w/o attention	53.7	49.1	57.2	49.9
MM-Pyramid (ours)	55.1	49.9	57.6	50.5

B.4. Positional encoding and temporal conv

Positional encoding is used for temporal modeling. Since the temporal convolution operation can provide temporal information, we do not add positional encoding for lower computation complexity. We added an ablated experiment for the role of positional encoding shown in Tab. 7, where “MM-Pyramid w/ PE” denotes adding additional positional encoding in each transformer unit, “MM-Pyramid w/o conv w/ PE” denotes replacing the temporal convolution block with positional encoding, and “MM-Pyramid w/o conv” denotes an ablated model where the convolution operations are removed. The results show that adding positional encoding to the MM-Pyramid module cannot bring more benefits for the performance, while using positional encoding as a substitution of the convolution block leads to

a slightly poor result. The results show that positional encoding is capable of providing temporal information yet the temporal convolution block performs better. As we mentioned before, the temporal convolution layer is able to provide feature amalgamation for semantic information construction, thus we argue that it is a better choice than positional encoding. The role of temporal order is significant for it tells the model the beginning, process, and end of a given event, which is important to generate event-related perception for better video understanding. The experimental results between the comparison of models with and without PE/temporal conv support our claims.

Table 7. Ablation studies on the positional encoding and temporal convolution.

Model	Type@AV		Event@AV	
	Seg	Eve	Seg	Eve
MM-Pyramid w/ PE	54.7	48.9	56.9	49.6
MM-Pyramid w/o conv w/ PE	53.4	47.7	56.3	48.4
MM-Pyramid w/o conv	53.1	47.0	56.4	47.8
MM-Pyramid (Full)	55.1	49.9	57.6	50.5

B.5. Comparison with pure transformer.

We provide the pure 4-layer uni-modal transformer model (denoted as Uni-Trans) and 4-layer uni-modal transformer encoder together with cross-modal transformer encoder (denoted as Hybr-Trans) model with or without positional encoding as additional ablated models on the LLP dataset. The related results are shown in Tab. 8, which show that our model achieves better results than the two ablated models, verifying the effectuality of our multimodal interaction and fusion strategy,

Table 8. Ablation studies on the transformer architectures

Model	Type@AV		Event@AV	
	Segment	Event	Segment	Event
Uni-Trans w/o PE	52.5	46.8	54.9	46.3
Uni-Trans w/ PE	52.9	46.7	55.2	46.1
Hybr-Trans w/o PE	54.3	47.9	55.8	48.2
Hybr-Trans w/ PE	54.5	47.6	56.1	48.5
MM-Pyramid (ours)	55.1	49.9	57.6	50.5

B.6. Impact of parameter sharing setting

To investigate the performance of the parameter sharing strategy of cross-modal attention blocks, we complement a non-sharing ablated model as shown in Tab. 9. The result indicates that the sharing matrices get comparable performance with lower computing complexity compared with the non-sharing setting.

Table 9. Segment-level and event-level f1-scores(%) comparison with different parameter sharing strategy.

Model	Type@AV		Event@AV	
	Segment	Event	Segment	Event
Non-Sharing	54.8	50.1	57.2	50.0
Sharing (ours)	55.1	49.9	57.6	50.5

B.7. Comparison with BigBird

The windowed attention in Fig. 1(b) of BigBird [48] is similar to our fixed-size attention mechanism. However, we argue that there remain at least two differences between our proposed module and the windowed attention proposed before. First, the size of the windowed attention is fixed in all transformer layers, while the size of our attention window is diverse in different layers. Second, the purpose of the windowed attention is to lower the complexity of the attention mechanism, while our fixed-size attention aims to obtain intra- and inter-modality interactions in different scales. Therefore, there are obvious distinctions between two mechanisms on the motivation (lower complexity vs. multi-scale interactions) and structure (fixed window size vs. dynamic window size).

C. Datasets Details

C.1. AVE Dataset

The Audio-Visual Event (AVE) dataset is a subset of AudioSet [12] containing 4,143 videos covering 29 categories. The audio-visual event in the dataset is at least 2s long. This dataset includes a wide range of domains including racing car, women speaking, chainsaw, etc. The author did not claim any license for the dataset and corresponding model. Since the dataset is open-sourced, the exploitation of the AVE dataset is permitted by the original proposer [37]. Besides, videos in the dataset do not contain any personally identifiable information or offensive content.

C.2. LLP Dataset

The Look, Listen, and Parse (LLP) dataset is an audio-visual video parsing dataset including 11,849 YouTube video clips. It is also a subset of AudioSet [12] and contains 25 categories such as vacuum cleaning, car running, singing. The AVVP project, including the dataset and corresponding method, is released under the GNU General Public License v3.0. The usage for research purposes of this dataset is permitted, and the data do not contain any personally identifiable information or offensive content.

D. Qualitative Results

D.1. Capability of capturing multiple events

We conduct more qualitative experiments on the audio-visual video parsing task in comparison with our ablated model “MM-Unpyramid”, where the sizes of all pyramid units are identical and equal to the size of the last pyramid units in our raw MM-Pyramid framework. Results shown in Fig. 7, Fig. 8, and Fig. 9 illustrate that our pyramid setting can detect more uni-modal and multimodal events in various lengths, while the “MM-Unpyramid” model fails to detect the accurate temporal boundaries, especially when the temporal length of the targeted event is relatively short.

D.2. Failure cases

Besides, we show a failure case of the audio-visual event localization task, which is shown in Fig. 10. Since multi-scale semantic information is captured, our model tends to mispredict some border segments of a long event. We argue that though the selective fusion block reduces the impact of irrelevant multi-level features, there is still a small amount of irrelevant information mixed in, resulting in a slightly poorer performance when localizing one-shot events.

We also show a failure case of the weakly-supervised audio-visual video parsing task on the LLP dataset. As shown in Fig. 11, our MM-Pyramid model can generate the correct predictions easily since the visual information changes drastically. However, our model performs unsatisfactorily on the audio predictions, where the audio events **dog** on the last second are neglected and the temporal boundary of **speech** is predicted incorrectly. We analyze that in the first second, the audio signal is relatively weak, while in the last second, the dog barking events vanish quickly. Therefore, it is hard for the pyramid units with the smallest size to capture these extremely short events, thereby causing such failure cases. One possible solution is to refine the visual and audio sample rates, which could change the second-level pyramid unit size to the frame-level size, leading to more detailed and accurate event recognition and localization results.

D.3. Role of selective fusion.

To illustrate the effectiveness of our selective fusion block in the attentive semantic fusion module, we conduct additional qualitative results as shown in Fig. 12. The sample video above the picture consists of some long audio and visual events as well as a small audio-visual event “speech”. Results show that the selective fusion module assigns relatively high scores on the pyramid units of large scales. It should be noticed that since the characteristics of pyramid features are not mutually exclusive, we use the sigmoid function as the substitution of softmax to generate fusion weights, thus the sum of weights is not 1. The sample video

below the picture consists of one visual event of medium length yet several audio events in various lengths. Therefore, the selective fusion block focuses more on the visual pyramid units with medium lengths and disperses weights into all audio pyramid units.

E. Limitation

Though our MM-Pyramid framework is capable of detecting multiple events in various lengths, the advantage is limited when detecting events that occur throughout the whole video compared with other methods. This can be shown in the experimental results of the audio-visual event localization task, in which task the majority (66.4%) of events span over the whole video. In that situation, we suggest that injecting our model or our multimodal pyramid feature methodology into other single-shot event detection methods as an enhancement for detecting multiple events.

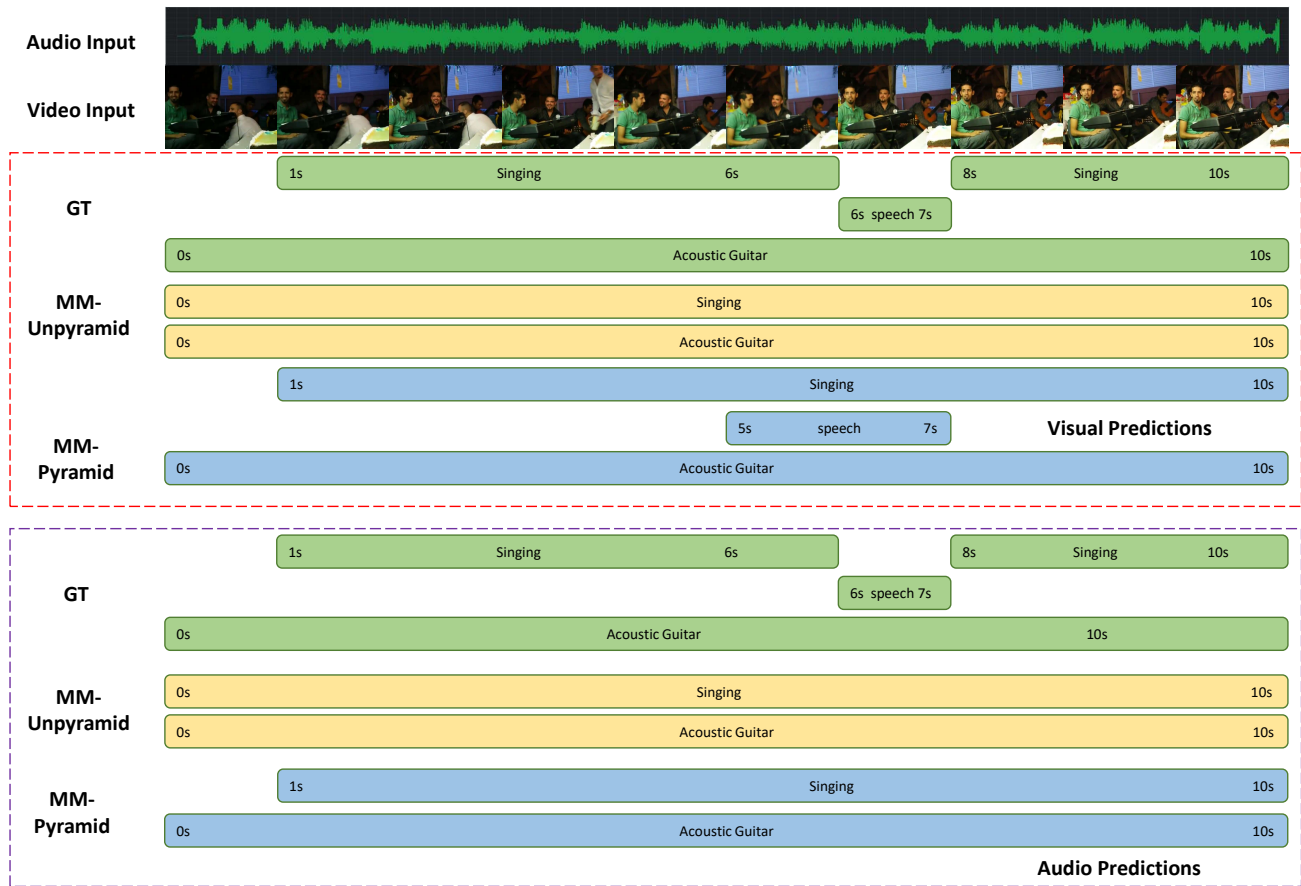


Figure 7. Qualitative comparison with the ablated model MM-Unpyramid. The red dotted box includes the visual predictions, and the audio predictions are in the purple dotted box. The green, yellow, and blue labels denote the ground-truth, predictions of MM-Unpyramid, and predictions of our MM-Pyramid, respectively.

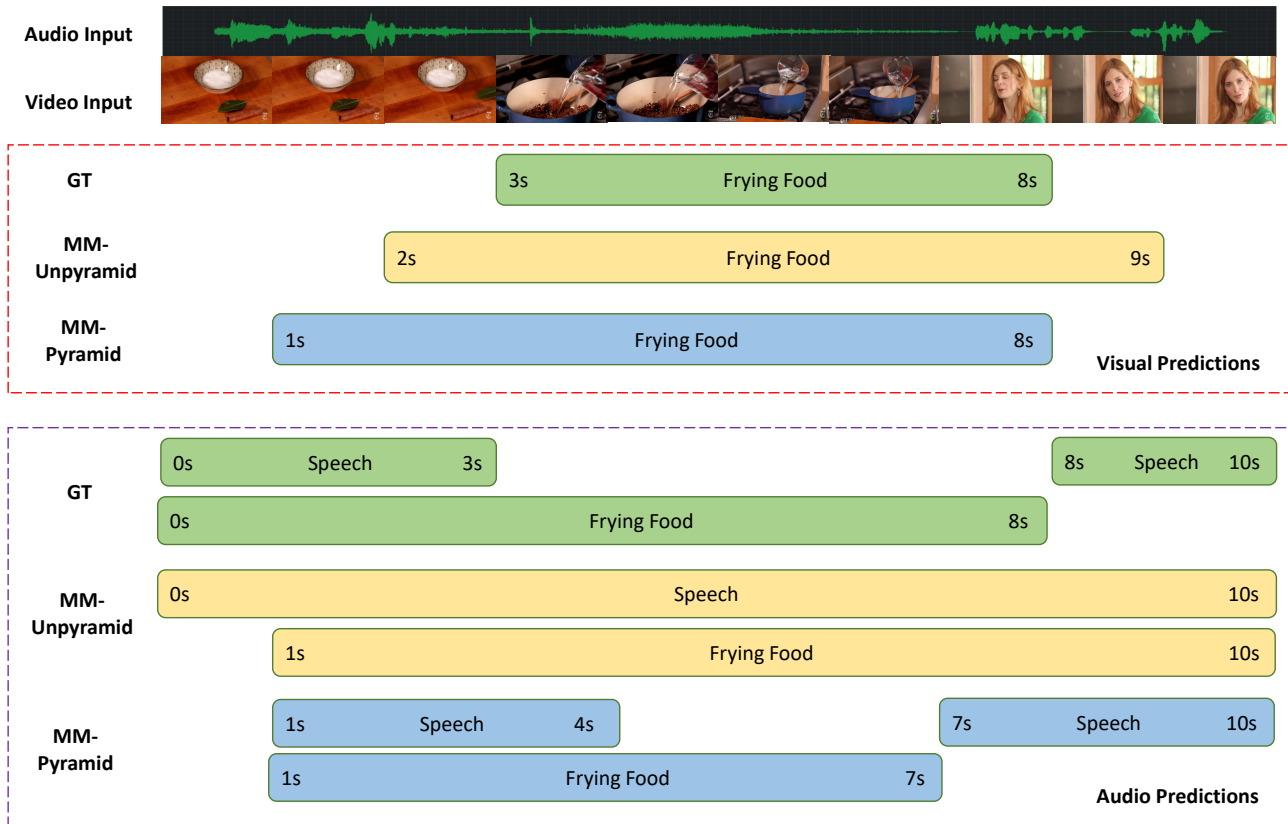


Figure 8. Qualitative comparison with the ablated model MM-Unpyramid. The red dotted box includes the visual predictions, and the audio predictions are in the purple dotted box. The green, yellow, and blue labels denote the ground-truth, predictions of MM-Unpyramid, and predictions of our MM-Pyramid, respectively.

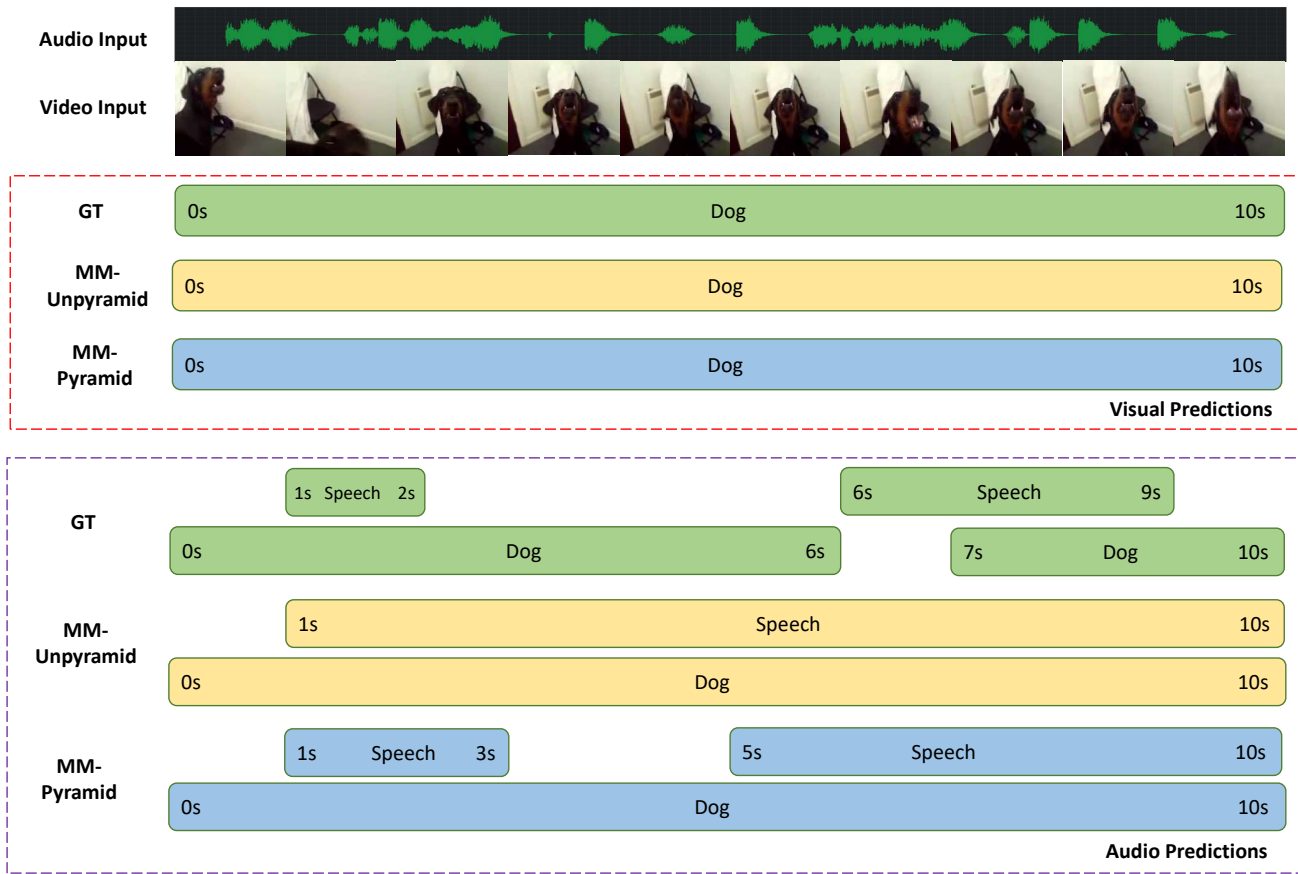


Figure 9. Qualitative comparison with the ablated model MM-Unpyramid. The red dotted box includes the visual predictions, and the audio predictions are in the purple dotted box. The green, yellow, and blue labels denote the ground-truth, predictions of MM-Unpyramid, and predictions of our MM-Pyramid, respectively.



Figure 10. Failure case on the audio-visual event localization task. Our model mispredicts the first and 9th-10th seconds as the “background”, which should be labeled as the “goat” event.

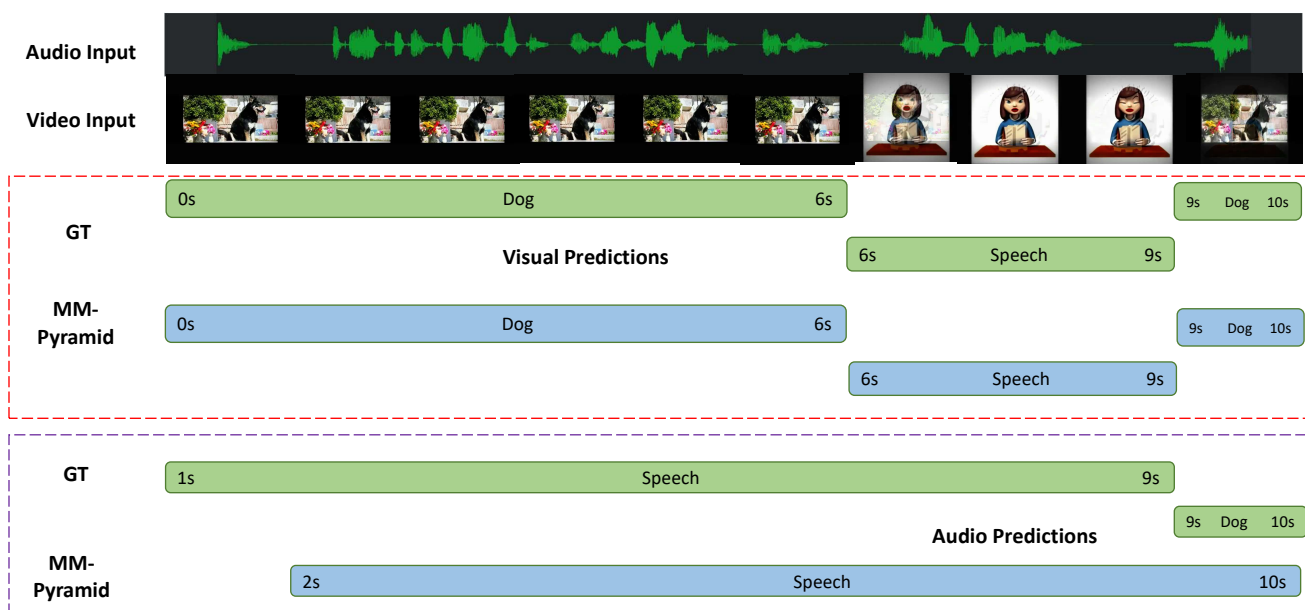


Figure 11. Failure case on the weakly-supervised audio-visual video parsing task. “GT” denotes the ground-truth. The red dotted box includes the visual predictions, and the audio predictions are in the purple dotted box.

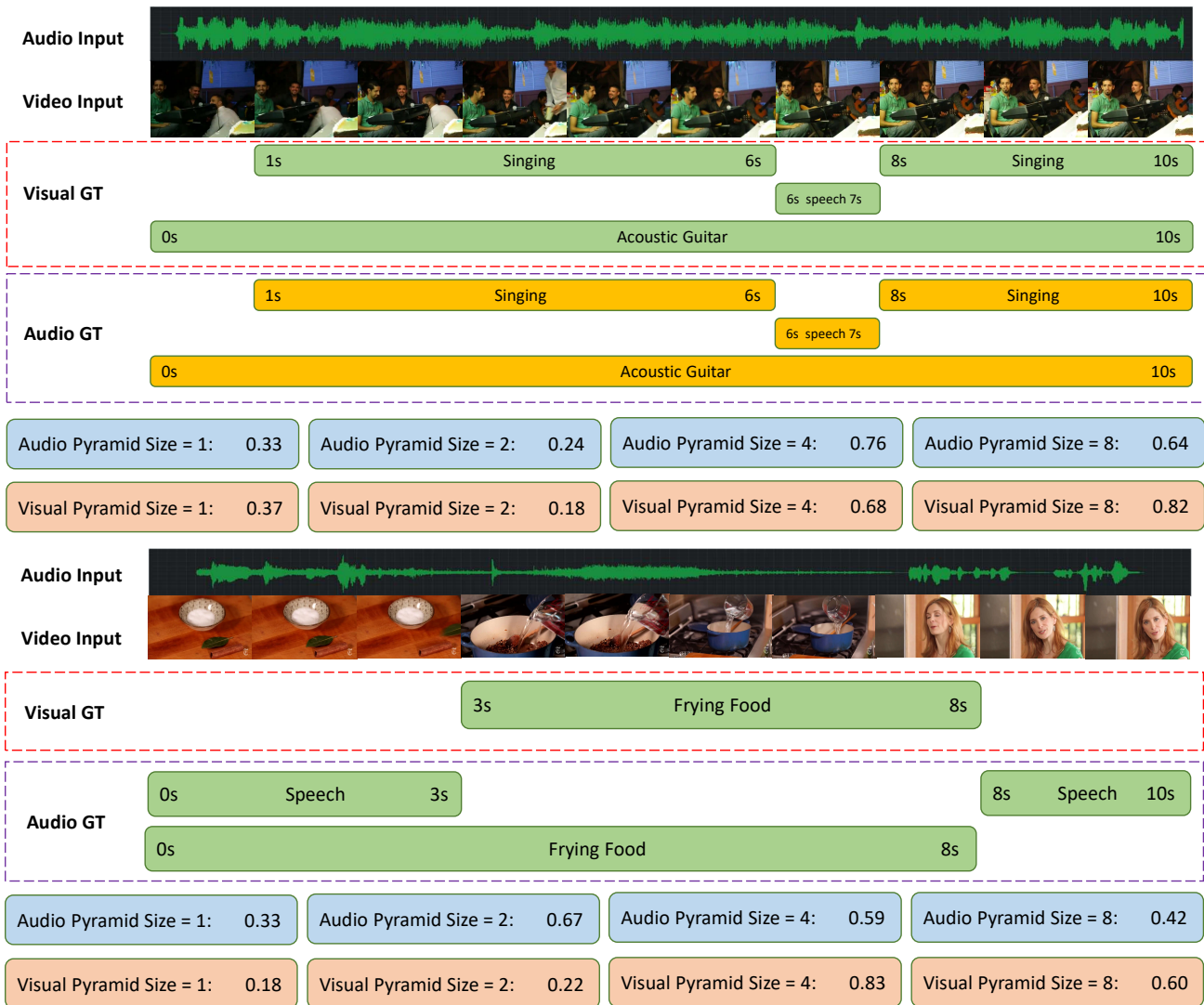


Figure 12. Qualitative results of the role of the selective fusion block, which assigns each pyramid unit weight for weighted sum calculation.